PNAS

Supplementary Information for

Microbiota-induced active translocation of peptidoglycan across the intestinal barrier dictates its within-host dissemination

Richard Wheeler[1#*], Paulo André Dias Bastos[1#], Olivier Disson[2$], Aline Rifflet[1$], Ilana Gabanyi[3,4], Julia Spielbauer[1], Marion Bérard[5], Marc Lecuit[2,6,7], Ivo Gomperts Boneca[1*]

Corresponding author(s): Ivo Gomperts Boneca, Richard Wheeler

Email: bonecai@pasteur.fr, wheelerrsci@gmail.com

This PDF file includes:

A

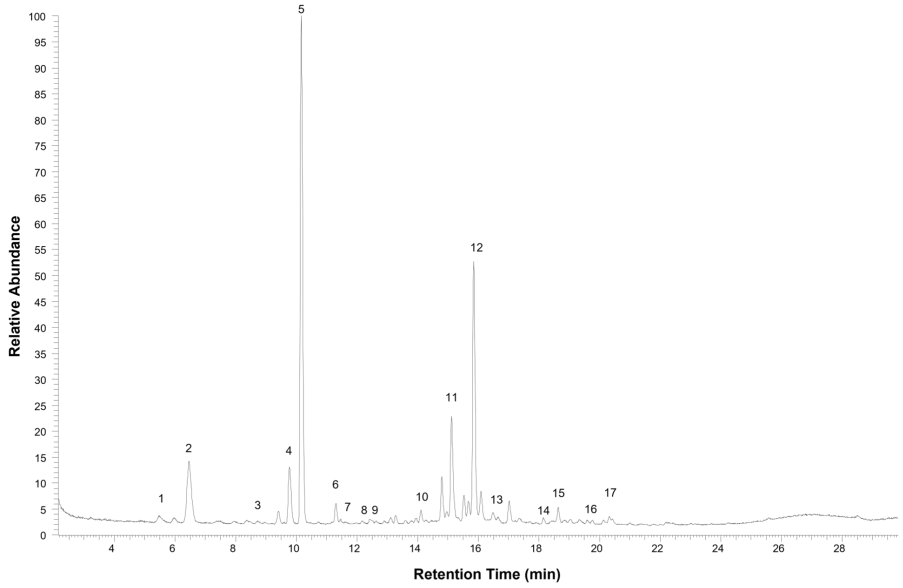

B

# peak	Muropeptide	Muropeptide Sequence	RT (min)	Formula	m/z observed	m/z theoretical	z	error ppm
1	GM3H	GM-AEmDapH	5,47	C40H65N9O21	504,7227	504,7220	2	1,39
2	GM3	GM-AEmDap	6,46	C34H58N6O20	436,1928	436,1926	2	0,46
3	GM4 (deAc GlcN)	GM-AEmDapA (deAc GlcN)	8,72	C35H61N7O20	450,7065	450,7059	2	1,33
4	GM2	GM-AE	9,82	C27H46N4O17	699,2932	699,2931	1	0,14
5	GM4	GM-AEmDapA	10,16	C37H63N7O21	471,7108	471,7111	2	-0,64
6	GM-GM4 (deAc GlcN)	GM-GM-AEmDapA (deAc GlcN)	11,28	C54H91N9O32	689,7962	689,7958	2	0,58
7	GM5	GM-AEmDapAA	11,44	C40H68N8O22	507,2308	507,2297	2	2,17
8	GM4-mDAPEA	GM-AEmDapA-mDapEA	12,18	C52H87N11O28	657,7946	657,7934	2	1,82
9	GM4-AmDAPEA	GM-AEmDapA-AmDapEA	12,43	C55H92N12O29	693,3129	693,3119	2	1,44
10	GM3-GM3	GM-AEmDap - GM-AEmDap	14,12	C68H114N12O39	862,3743	862,3726	2	1,97
11	GM3-GM4	GM-AEmDap - GM-AEmDapA	15,12	C71H119N13O40	897,8924	897,8911	2	1,45
12	GM4-GM4	GM-AEmDapA - GM-AEmDapA	15,86	C74H124N14O41	933,4109	933,4097	2	1,29
13	GanhM4	GanhM-AEmDapA	16,50	C37H59N7O20	922,3901	922,3888	1	1,41
14	GM3-GM4-GM4	GM-AEmDap - GM-AEmDapA - GM-AEmDapA	18,15	C108H180N20O60	906,7312	906,7289	3	2,54
15	GM4-GM4-GM4	GM-AEmDapA - GM-AEmDapA - GM-AEmDapA	18,65	C111H185N21O61	930,4108	930,4079	3	3,12
16	GanhM3-GanhM4	GanhM-AEmDap - GanhM-AEmDapA	19,60	C71H115N13O39	887,8800	887,8780	2	2,25
17	GanhM4-GM4	GanhM-AEmDapA - GM-AEmDapA	20,33	C74H120N14O40	923,3984	923,3966	2	1,95

Fig. S1. Relative abundance of *E. coli* muropeptides A) UHPLC profile indicating the relative abundance of muropeptides from a typical *Escherichia coli* peptidoglycan preparation. Numbered peaks are identified in the table below. B) Summary table of muropeptides identified by mass spectrometry. G, *N*-acetyl-glucosamine; M, *N*-acetyl-muramitol (reduced form of *N*-acetyl-muramic acid); anhM, 1,6-anhydro-*N*-acetylmuramic acid; 2-5, peptide stem length; A, alanine; E, isoglutamate; mDap, meso-diaminopimelic acid; H, histidine; deAc GlcN, *N*-deacetylated glucosamine.

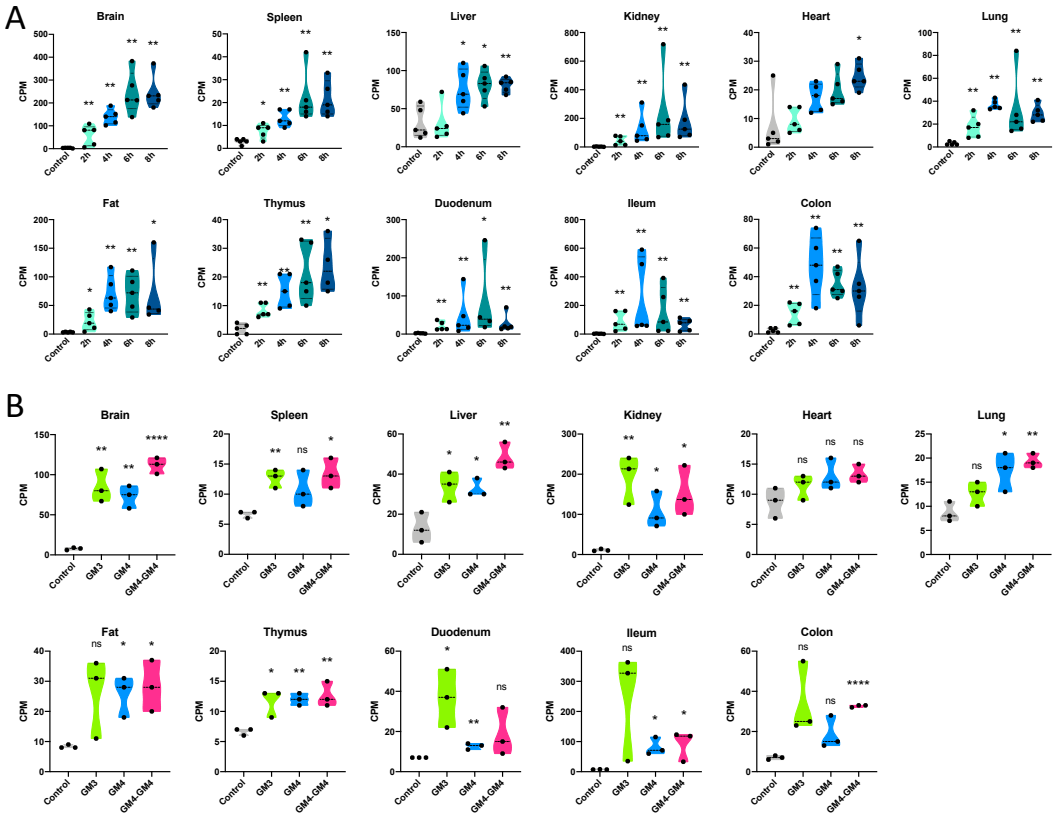

Fig. S2. The kinetics of [3H]-PGN biodistribution following *per os* administration in mice. A) [^{3}H]-PGN measured by scintillation counting of dissolved, decolored organs and blood between 2h and 8 h post-gavage. Data are presented as CPM per whole organ, or per tissue fragment (duodenum, ileum, colon). Welch's ANOVA comparing time-point groups, excluding control: Brain $P = 0.0564$; Spleen $P = 0.5902$; Liver $P = 0.0895$; Kidney $P = 0.2958$; Heart $P = 0.5178$; Lung $P = 0.0656$; Fat $P = 0.9250$; Duodenum $P = 0.1740$; Ileum $P = 0.4658$; Colon $P = 0.1766$. Pairwise comparisons to control performed using the Mann–Whitney U test. * $P \leq 0.05$; ** $P \leq 0.005$; *** $P \leq 0.0005$. B) The biodistribution of [^{3}H]-GM3, [^{3}H]-GM4 and [^{3}H]-GM4-GM4, administered *per os* in SPF mice. Data are presented as CPM per whole organ, or per tissue fragment. Pairwise comparison with control performed using unpaired t-test. * $P \leq 0.05$; ** $P \leq 0.0050$; *** $P \leq 0.0005$; $P < 0.0001$. Welch's ANOVA comparing muropeptides groups, excluding control: Brain $P = 0.0564$; Spleen $P = 0.5902$; Liver $P = 0.0895$; Kidney $P = 0.2958$; Heart $P = 0.7861$; Lung $P = 0.0656$; Fat $P = 0.0925$; Thymus $P = 0.8678$; Duodenum $P = 0.1740$; Ileum $P = 0.4658$; Colon $P = 0.1766$.

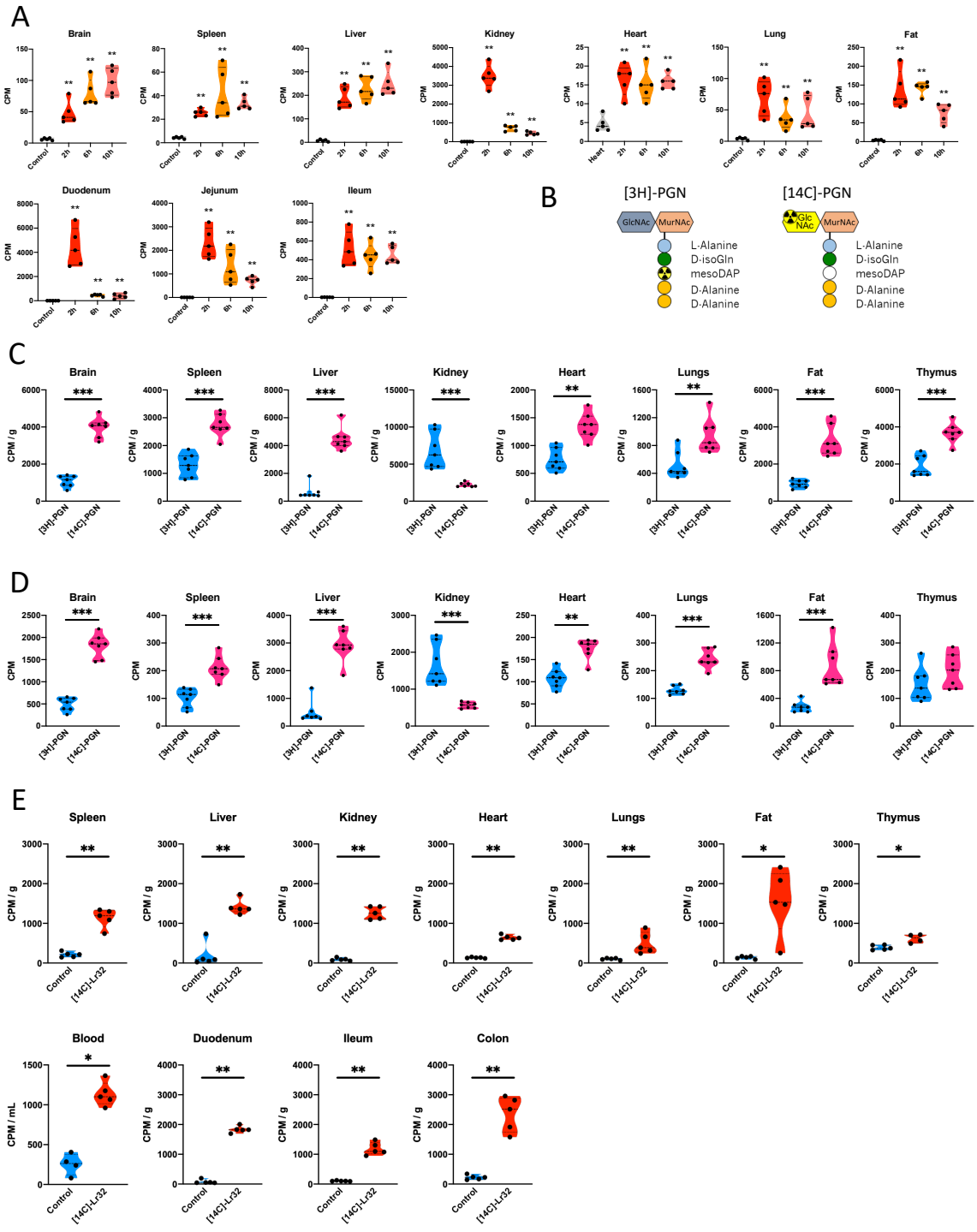

Fig. S3. Effect of labelling strategy parameters on biodistribution of peptidoglycan. A) Biodistribution of [^{3}H]-mesoDAP amino acid administered to mice *per os*. [^{3}H]-mesoDAP biodistribution was measured by scintillation counting of dissolved, decolored organs, 2h, 6h and 10 h post-gavage. Data are presented as CPM per whole organ or tissue fragment. Welch's ANOVA comparing time-point groups, excluding control: Brain P = 0.0159; Spleen P = 0.0529; Liver P = 0.2269; Kidney P < 0.0001; Heart P = 0.8868; Lung P = 0.1827; Fat P = 0.0066; Duodenum P = 0.0054; Jejunum P = 0.0056; Ileum P = 0.7670. B) Schematic summary of

radiolabeling methodology, indicating the position of the 3H-labelled mesoDAP and 14C-labelled GlcNAc. C) Biodistribution of [^{3}H]-PGN versus [^{14}C]-PGN administered to mice *per os*. Mice were gavaged with 400,000 cpm of [^{3}H]-PGN or [^{14}C]-PGN and scintillation counting performed on dissolved, decolored organs 4h post gavage. Data normalized as CPM values per g tissue weight. D) [^{3}H]-PGN or [^{14}C]-PGN biodistribution data presented as CPM per whole organ, or per tissue fragment without normalization. E) Biodistribution of [^{14}C]-PGN from *L. rhamnosus* Lr32, 4h after administration to mice *per os*. Data normalized as CPM values per g tissue weight. Pairwise comparison to control performed using the Mann–Whitney U test. * $P \leq 0.05$; ** $P \leq 0.005$; *** $P \leq 0.0005$.

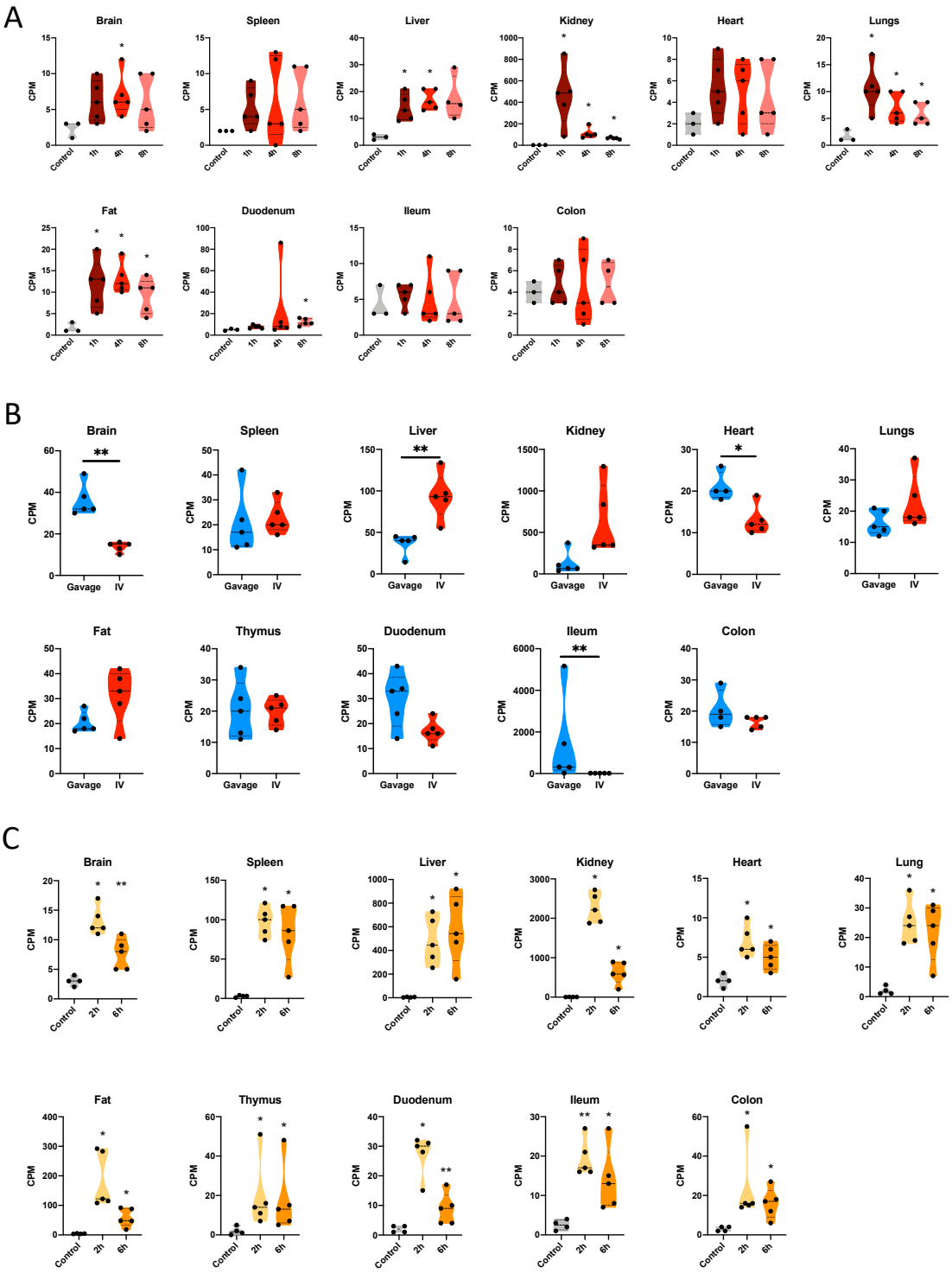

Fig. S4. Biodistribution of different doses of [^{3}H]-PGN following intravenous or intraperitoneal administration, without tissue weight normalization. A) Mice were administered 40,000 CPM of [3H]-PGN intravenously and biodistribution to organs and tissues measured at 1h, 4h, 8h and 24h post-injection. Welch's ANOVA comparing time-point groups, excluding control: Brain $P = 0.8823$; Spleen $P = 0.8644$; Liver $P = 0.5885$; Kidney $P < 0.0370$; Heart

P = 0.9196; Lung P = 0.1599; Fat P = 0.3361; Duodenum P = 0.0758; Ileum P = 0.9186; Colon P = 0.9833. B) Comparison of [3H]-PGN distribution administered intravenously versus gavage. Mice were administered 400,000 CPM of [3H]-PGN intravenously or by gavage, and biodistribution to organs and tissues assessed at 1h (intravenous) or 4h (gavage). C) Biodistribution of [^{3}H]-PGN administered intraperitoneally. Mice were injected intraperitoneally with 400,000 CPM of [^{3}H]-PGN and by scintillation counting performed on the dissolved, decolored organs harvested at 2h and 6h post-gavage. Pairwise comparison with between time-points performed using the Mann–Whitney U test, Brain P = 0.0159; Spleen P = 0.6508; Liver P = 0.5476; Kidney P = 0.0079; Heart P = 0.1667; Lung P = 0.8095; Fat P = 0.0079; Duodenum P = 0.0159; Ileum P = 0.1190; Colon P = 0.9365. Pairwise comparison to control performed using the Mann–Whitney U test. * $P \leq 0.05$; ** $P \leq 0.005$; *** $P \leq 0.0005$.

A

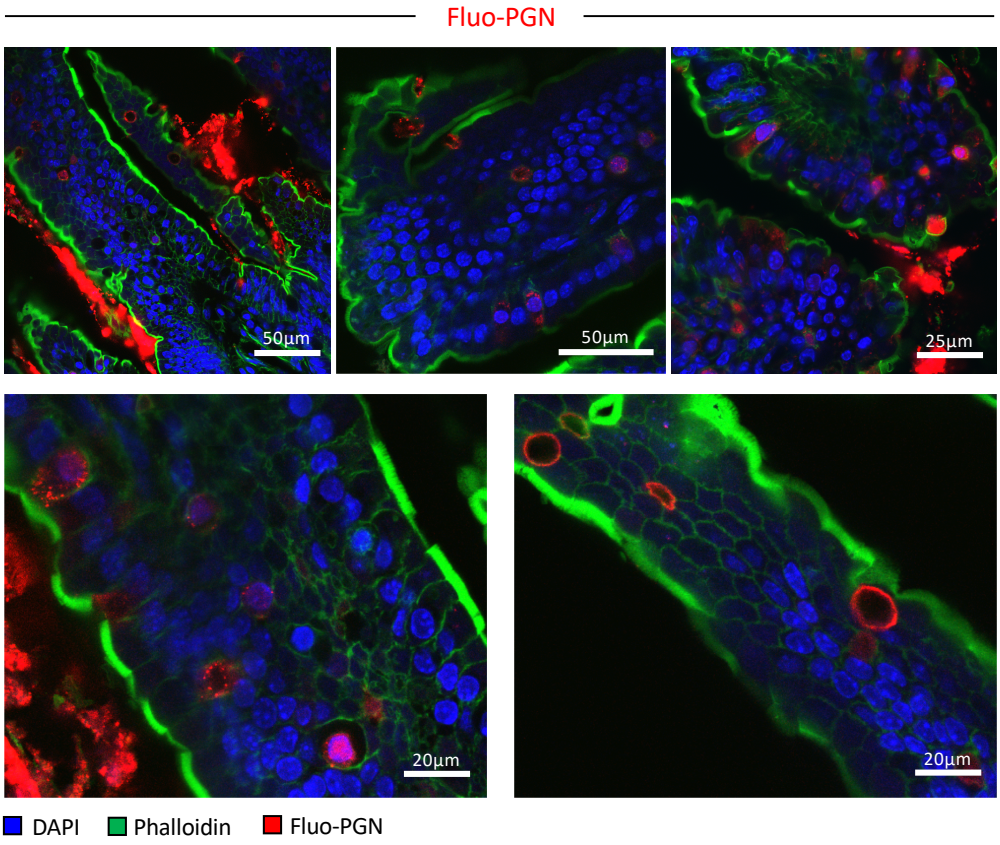
Fluo-PGN
50μm
50μm
25μm
20μm
20μm
DAPI
Phalloidin
Fluo-PGN
Vehicle
50μm
50μm
25μm
DAPI
Phalloidin
Fluo-PGN

80

B

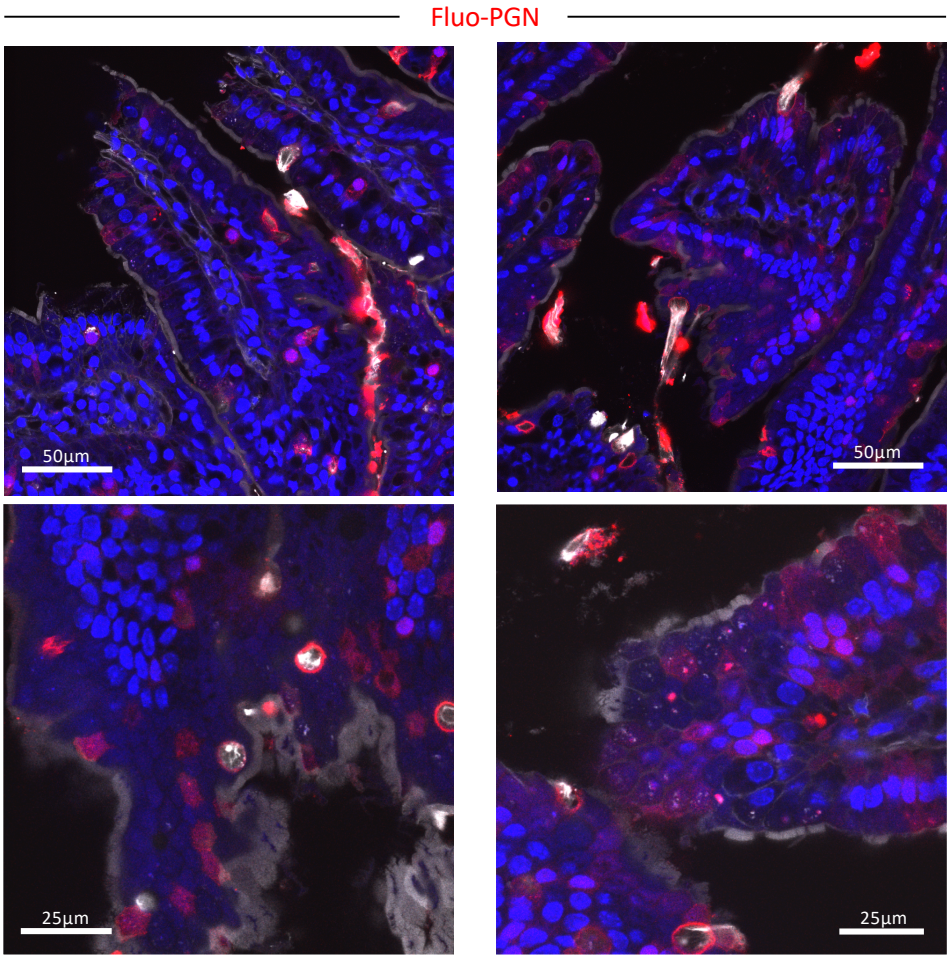
Fluo-PGN
50µm
50µm
25µm
25µm
DAPI
Fluo-PGN
WGA
Vehicle
50µm
50µm
DAPI
Fluo-PGN
WGA

81

82

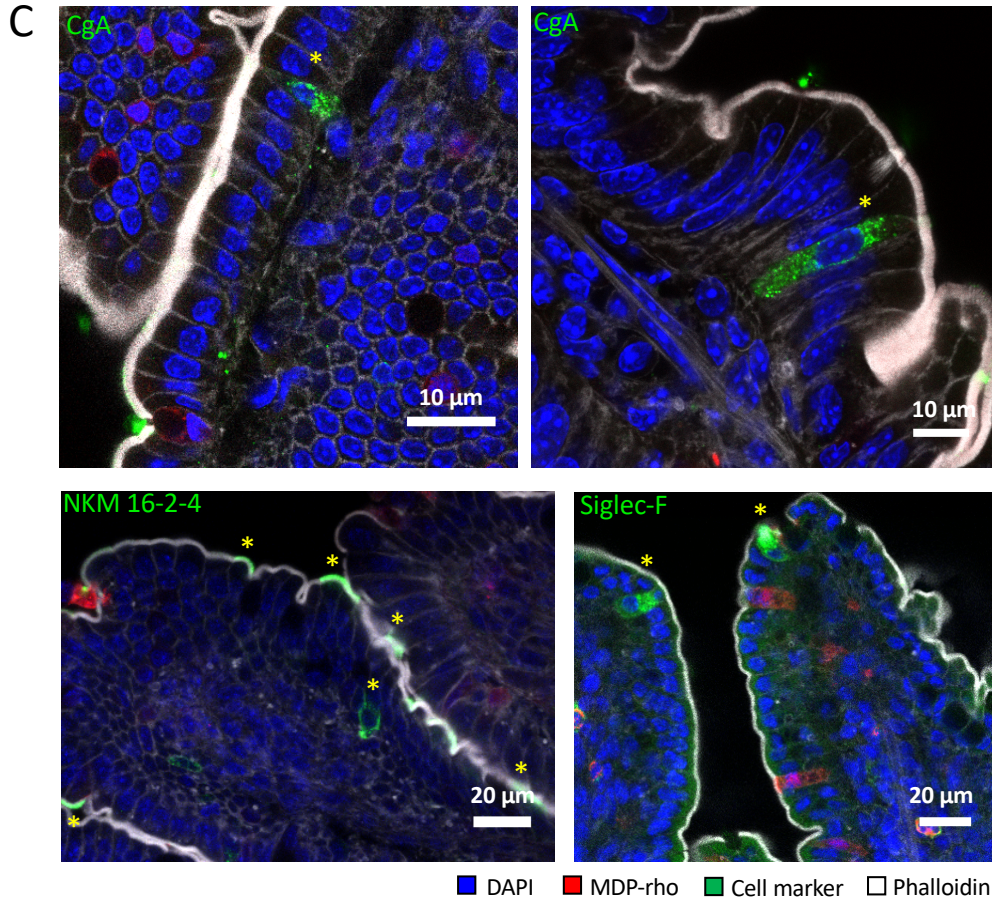

Fig. S5. Cellular localization of fluorescently labelled peptidoglycan in the mouse ileal epithelium. A) Internalization of peptidoglycan-AF647 conjugate (Fluo-PGN) in the ileum of SPF mice by a subset of epithelial cells. B) Fluo-PGN internalized in villus epithelial cells largely colocalizes with Wheat Germ Agglutinin (WGA) stained goblet cells C) MDP-rho uptake assessed in enteroendocrine cells, M cells and tuft cells. No association with MDP-rho was observed for CgA^+ enteroendocrine cells, NKM-16-4-2^+ M cells or Siglec-F^+ tuft cells (green staining), whereas MDP-rho uptake is observed elsewhere in the same field. Yellow asterisks highlight antibody positive cells in each panel.

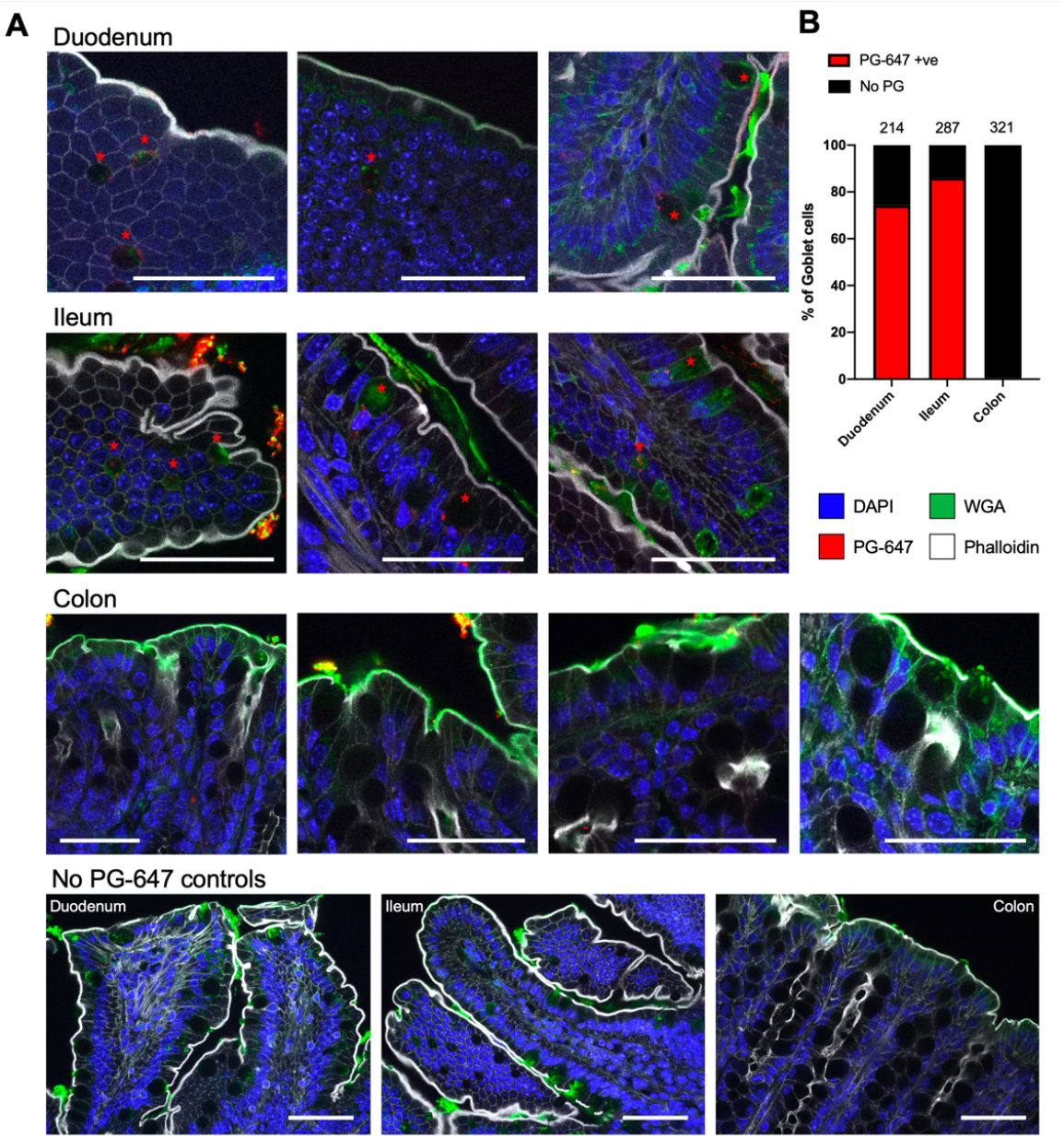

Fig. S6. Uptake of peptidoglycan by goblet cells in different regions of the intestinal tract. A) Intestinal ligatures were prepared in the duodenum, ileum and colon of mice, and injected with *E. coli* peptidoglycan AlexaFluor 647 conjugate (PG-647; red), or PBS (No PG-647 controls; bottom row). Scale bars = 50 μm. Counter staining is with DAPI (blue), Wheat-Germ Agglutinin Alexa Fluor 488 conjugate (WGA; green) and Phalloidin iFluor 555 conjugate (white). Red stars indicate goblet cells where internalized PG-647 is visible in the image. B) Percentage of goblet cells in each region displaying uptake or not of PG-647. For each region, the number above each bar indicates the number of goblet cells counted.

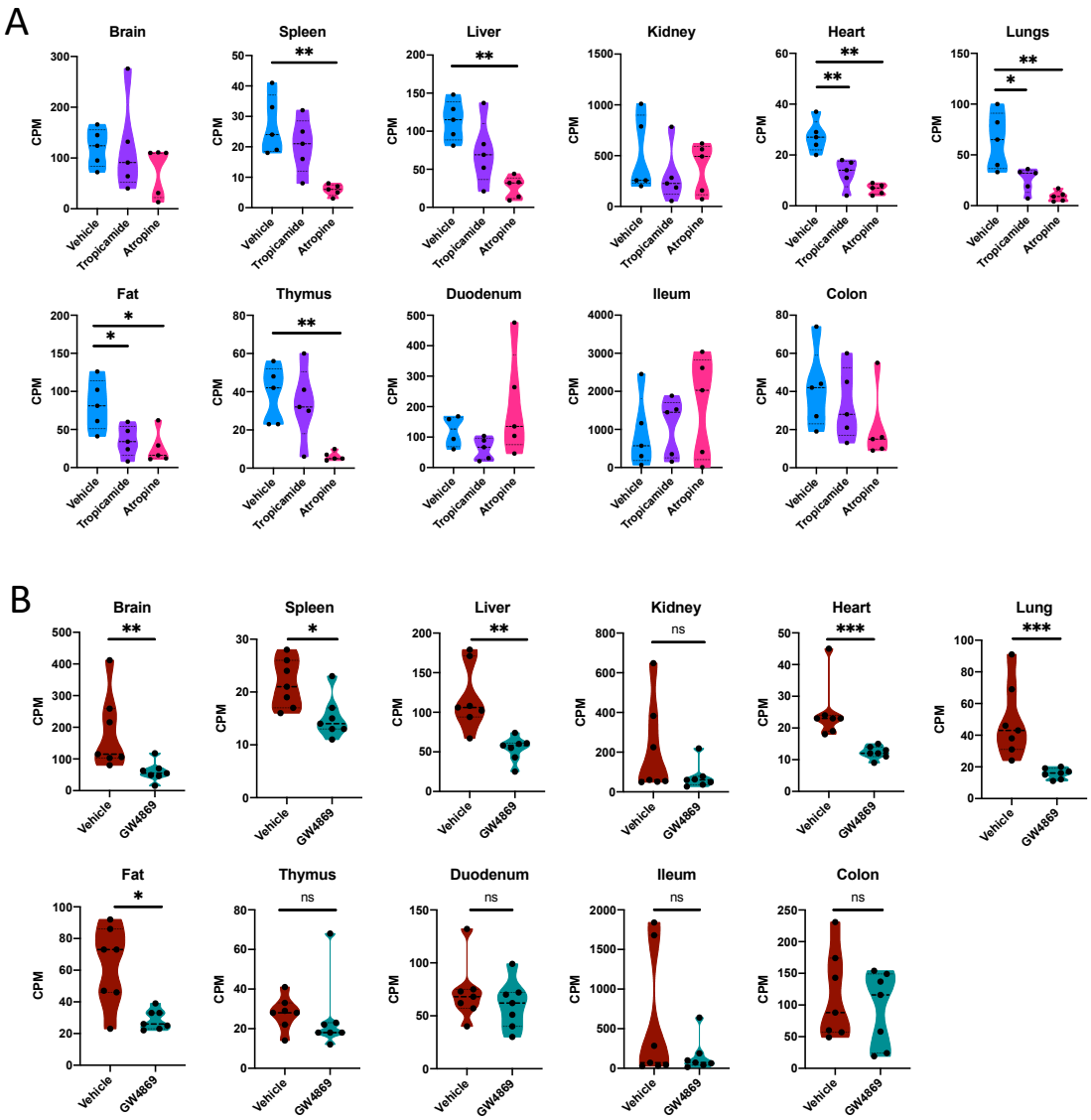

Fig. S7. Regulation of the dissemination of [3H]-PGN across the gut. A) Muscarinic receptor antagonism suppresses the systemic biodistribution of [3H]-PGN without normalization. SPF mice were administered tropicamide, atropine or vehicle control prior to gavage with [^{3}H]-PGN. Scintillation counting was performed on dissolved, decolored organs. Results are presented as CPM per whole organ, per tissue fragment (duodenum, ileum and colon). B) [^{3}H]-PGN biodistribution from the gut is suppressed by GW4869 treatment. Results are presented as CPM per whole organ, per tissue fragment (duodenum, ileum and colon). Pairwise comparison to vehicle control performed using the Mann–Whitney U test. * $P \leq 0.05$; ** $P \leq 0.005$.

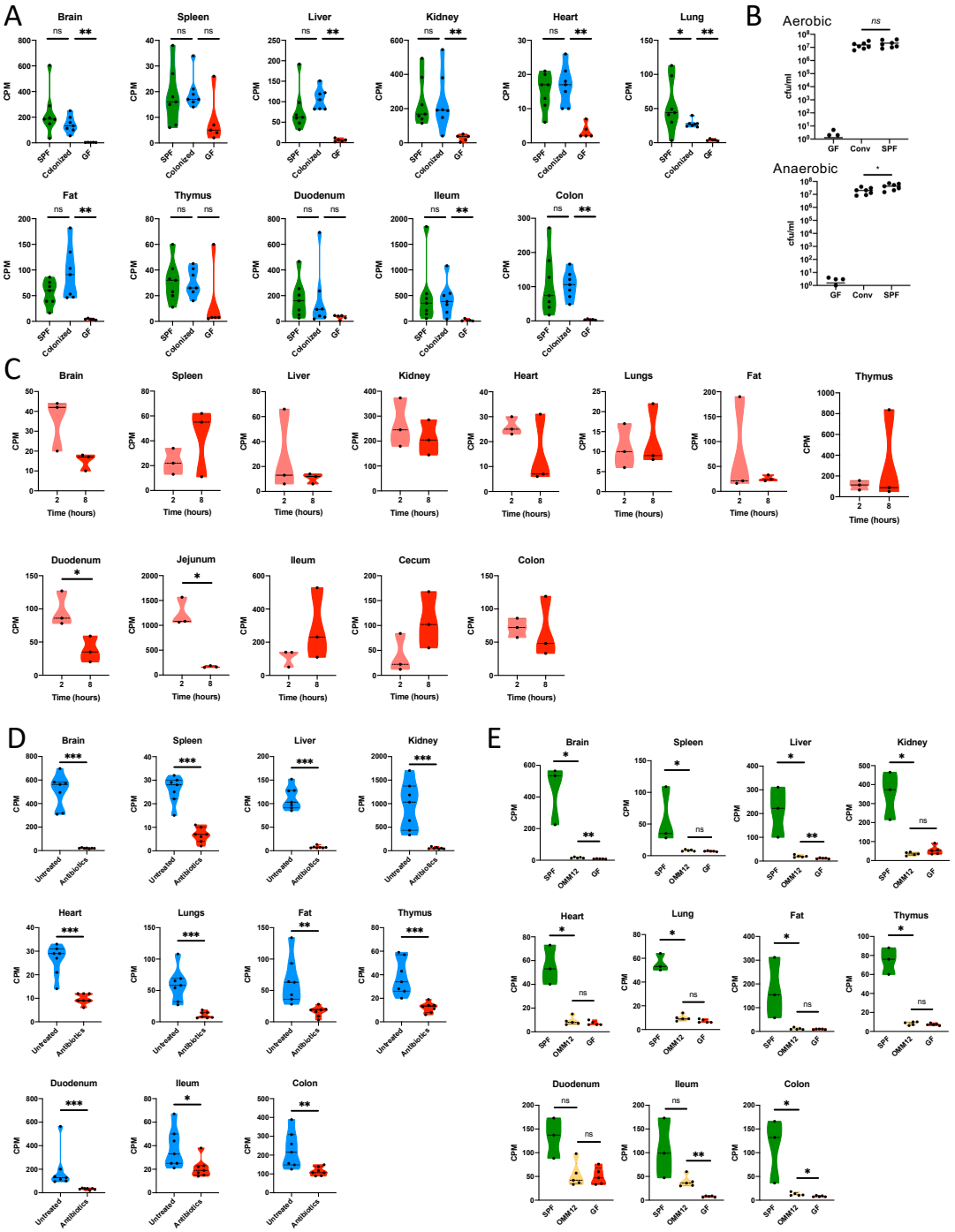

Fig. S8. Dependency of [3H]-PGN biodistribution on microbial colonization status of the host. A) The biodistribution of [^{3}H]-PGN in germ-free (GF) mice, specific pathogen free (SPF) mice and conventionalized mice (previously GF mice co-housed with SPF for 3 weeks) presented as CPM per whole organ, or per tissue fragment (duodenum, ileum, colon). B) Enumeration of aerobically and anaerobically cultured fecal microbiota from germ-free, conventionalized and SPF mice. Feces were collected immediately prior to gavage with [^{3}H]-PGN. C) The biodistribution of [^{3}H]-PGN in germ-free mice 2h and 8h post gavage. D) Biodistribution of [3H]-PGN in SPF mice treated with a broad-spectrum antibiotic cocktail. E) Biodistribution of [^{3}H]-PGN in SPF mice,

OMM12 mice and GF mice presented as CPM per whole organ, or per tissue fragment (duodenum, ileum, colon). A, B, D and E) Pairwise comparisons performed using the Mann–Whitney U test. * $P \leq 0.05$; ** $P \leq 0.005$; *** $P \leq 0.0005$. C) Pairwise comparisons performed using Welch's t-test. * $P \leq 0.05$.

Table S1. Summary table of selected muropeptides detected from peptidoglycan of the mouse gut microbiota. Muropeptide composition of the gut microbiota of four female C57BL/6J mice was assessed. A selection of 60 muropeptides were targeted, belonging to types A1α, A1γ and A4α, expected to be abundant among members of the gut microbiota.[1] Analysis was by LC-MS. For each muropeptide, the identity was confirmed by analysis of MS2 spectra. Muropeptides are grouped according to the characteristic diamino acid present at position 3 of the peptide stem, and color coded according to Fig. 1: blue, meso-diaminopimelic acid; green, amidated meso-diaminopimelic acid; red, lysine; white, muramyl dipeptide (no amino acid at position 3). G, N-acetyl-glucosamine; GlcN, N-deacetylated glucosamine; M, N-acetyl-muramitol (reduced form of N-acetyl-muramic acid); anhM, 1,6-anhydro-N-acetylmuramic acid; A, alanine; E, isoglutamate; Q, isoglutamine; mDap, meso-diaminopimelic acid; mDapNH2, amidated meso-diaminopimelic acid; K, lysine; N, asparagine; D, aspartic acid. Subscript Q indicates isoglutamine is presented instead of isoglutamate for muropeptides with mesoDAP or amidated mesoDAP at position 3 of the peptide stem.

Muropeptide	Plot Name (Fig. 1)	Retention Time (min)	Formula	Neutral Mass	m/z theoretical	m/z observed	z	error ppm
GM-AE	GM2	8.91	C27H46N4O17	698.29	699.2931	699.2924	1	-1.00
GM-AQ	$GM2_Q$	7.11	C27H47N5O16	697.30	698.3091	698.3086	1	-0.72
GanhM-AE	GanhM2	17.00	C27H42N4O16	678.26	679.2669	679.2684	1	2.21
GanhM-AQ	$GanhM2_Q$	15.85	C27H43N5O15	677.28	678.2828	678.2831	1	0.44
GM-AEmDap	GM3	5.79	C34H58N6O20	870.37	436.1926	436.1925	2	-0.23
GM-AEmDap (deAc GlcN)	GM3*	4.05	C32H56N6O19	828.36	415.1864	415.1876	2	2.89
GM-AQmDap	$GM3_Q$	4.62	C34H59N7O19	869.39	435.7005	435.7013	2	1.84
GM-AQmDap (deAc GlcN)	$GM3_Q$*	3.10	C32H57N7O18	827.38	414.6952	414.6957	2	1.21
GM-AEmDapA	GM4	9.47	C37H63N7O21	941.41	471.7111	471.7116	2	1.06
GM-AEmDapA (deAc GlcN)	GM4*	7.90	C35H61N7O20	899.40	450.7059	450.7062	2	0.67
GM-AQmDapA	$GM4_Q$	8.46	C37H64N8O20	940.42	471.2191	471.2196	2	1.06
GM-AQmDapA (deAc GlcN)	$GM4_Q$*	6.00	C35H62N8O19	898.41	450.2138	450.2145	2	1.55
GM-AEmDapAA	GM5	10.92	C40H68N8O22	1012.44	507.2297	507.2307	2	1.97
GanhM-AEmDap	GanhM3	13.65	C34H54N6O19	850.34	851.3515	851.3530	1	1.76
GanhM-AEmDapA	GanhM4	16.20	C37H59N7O20	921.38	922.3888	922.3905	1	1.84
GM-AEmDap - GM-AEmDap	GM3-GM3	14.00	C68H114N12O39	1722.73	862.3723	862.3750	2	3.13
GM-AEmDap - GM-AEmDap (deAc GlcN 1x)	GM3-GM3*	13.12	C66H112N12O38	1680.72	841.3673	841.3686	2	1.55
GM-AEmDap - GM-AEmDapA	GM3-GM4	14.80	C71H119N13O40	1793.77	897.8911	897.8931	2	2.23
GM-AEmDap - GM-AEmDapA (deAc GlcN 1x)	GM3-GM4*	14.00	C69H117N13O39	1751.76	876.8867	876.8877	2	1.14
GM-AQmDap - GM-AQmDapA	$GM3-GM4_Q$	14.05	C71H121N15O38	1791.80	896.9071	896.9089	2	2.01
GM-AEmDapA - GM-AEmDapA	GM4-GM4	15.75	C74H124N14O41	1864.80	933.4097	933.4116	2	2.04
GM-AEmDapA - GM-AEmDapA (deAc GlcN 1x)	GM4-GM4*	14.80	C72H122N14O40	1822.79	912.4059	912.4063	2	0.44
GM-AQmDapA - GM-AQmDapA	$GM4-GM4_Q$	14.80	C74H126N16O39	1862.84	932.4257	932.4271	2	1.50
GM-AEmDapNH_2	GM3	5.00	C34H59N7O19	869.39	435.7006	435.7010	2	0.92
GM-AEmDapNH_2 (deAc GlcN)	GM3*	3.40	C32H57N7O18	827.38	414.6953	414.6958	2	1.21
GM-AQmDapNH_2	$GM3_Q$	4.00	C34H60N8O18	868.40	435.2086	435.2089	2	0.69
GM-AQmDapNH_2 (deAc GlcN)	$GM3_Q$*	2.72	C32H58N8O17	826.39	414.2033	414.2035	2	0.48
GM-AEmDapNH_2A	GM4	-	C37H64N8O20	940.42	471.2191	ND	2	-
GM-AEmDapNH_2A (deAc GlcN)	GM4*	7.20	C35H62N8O19	898.41	450.2138	450.2141	2	0.67
GM-AQmDapNH_2A	$GM4_Q$	8.00	C37H65N9O19	939.44	470.7271	470.7275	2	0.85
GM-AQmDapNH_2A deAc	$GM4_Q$*	4.40	C35H63N9O18	897.43	449.7218	449.7224	2	1.33
GM-AEmDapNH_2 - GM-AEmDapNH_2A	GM3-GM4	-	C71H121N15O38	1791.80	896.9071	ND	2	-
GM-AQmDapNH_2 - GM-AQmDapNH_2A	$GM3-GM4_Q$	12.50	C71H123N17O36	1789.83	895.9231	895.9241	2	1.12
GM-AEmDapNH_2A - GM-AEmDapNH_2A	GM4-GM4	14.50	C74H126N16O39	1862.84	932.4257	932.4294	2	3.97
GM-AQmDapNH_2A - GM-AQmDapNH_2A	$GM4-GM4_Q$	13.50	C74H128N18O37	1860.87	931.4417	931.4431	2	1.50
GM-AQK	GM3	5.62	C33H59N7O17	825.40	413.7056	413.7061	2	1.21
GM-AQKN	GM3N	10.15	C37H65N9O19	939.44	470.7271	470.7279	2	1.70
GM-AQKD	GM3D	10.75	C37H64N8O20	940.42	471.2191	471.2197	2	1.27
GM-AQKA	GM4	9.22	C36H64N8O18	896.43	449.2242	449.2246	2	0.89
GM-AQKAN	GM4N	11.80	C40H70N10O20	1010.48	506.2457	506.2465	2	1.58
GM-AQKAD	GM4D	12.27	C40H69N9O21	1011.46	506.7377	506.7386	2	1.78
GM-AQKAA	GM5	10.33	C39H69N9O19	967.47	484.7428	484.7433	2	1.03
GM-AQKAAN	GM5N	12.33	C43H75N11O21	1081.51	541.7642	541.7650	2	1.48
GM-AQKAAD	GM5D	12.85	C43H74N10O22	1082.50	542.2562	542.2571	2	1.66
GM-AQKN - GM-AQKA	GM3N-GM4	15.11	C73H127N17O36	1817.86	909.9388	909.9404	2	1.76
GM-AQKN - GM-AQKAN	GM3N-GM4N	16.31	C77H133N19O38	1931.91	644.9759	644.9774	3	2.33
GM-AQKN - GM-AQKAD	GM3N-GM4D	16.84	C77H132N18O39	1932.89	645.3039	645.3055	3	2.48
GM-AQKAN - GM-AQKA	GM4N-GM4	16.21	C76H132N18O37	1888.90	945.4573	945.4595	2	2.33
GM-AQKAN - GM-AQKAN	GM4N-GM4N	17.42	C80H138N20O39	2002.94	668.6549	668.6564	3	2.24
GM-AQKAN - GM-AQKAD	GM4N-GM4D	17.95	C80H137N19O40	2003.93	668.9829	668.9844	3	2.24
GM-AQKAAN - GM-AQKA	GM5N-GM4	16.50	C79H137N19O38	1959.94	654.3197	654.3207	3	1.53
GM-AQKAAN - GM-AQKAN	GM5N-GM4N	17.60	C83H143N21O40	2073.98	692.3340	692.3355	3	2.17
GM-AQKAAN - GM-AQKAD	GM5N-GM4D	18.20	C83H142N20O41	2074.96	692.6620	692.6631	3	1.59
GM-AQKAAD - GM-AQKAD	GM5D-GM4D	18.60	C83H141N19O42	2075.95	692.9900	692.9919	3	2.74
GM-AQKN - GM-AQKAN- GM-AQKAN	GM3N-GM4N-GM4N	19.40	C117H201N29O57	2924.37	975.7980	975.7997	3	1.74
GM-AQKN - GM-AQKAN- GM-AQKAD	GM3N-GM4N-GM4D	19.90	C117H200N28O58	2925.36	976.1260	976.1285	3	2.56
GM-AQKAN - GM-AQKAN- GM-AQKAN	GM4N-GM4N-GM4N	20.27	C120H206N30O58	2995.41	999.4770	999.4789	3	1.90
GM-AQKAN - GM-AQKAN- GM-AQKAD	GM4N-GM4N-GM4D	20.80	C120H205N29O59	2996.39	999.8050	999.8082	3	3.20
GM-AQKAAN - GM-AQKAN- GM-AQKAN	GM5N-GM4N-GM4N	20.40	C123H211N31O59	3066.45	1023.1560	1023.1588	3	2.74
GM-AQKAAN - GM-AQKAN- GM-AQKAD	GM5N-GM4N-GM4D	20.90	C123H210N30O60	3067.43	1023.4841	1023.4871	3	2.93

Supplementary Information References

1. Schleifer, K. H. & Kandler, O. Peptidoglycan types of bacterial cell walls and their taxonomic implications. Bacteriol. Rev. 36, 407–477 (1972).